

SHORT COMMUNICATION

Focal Adjustment for Star Tracker

Hai-bo Liu^{*}, Jian-kun Yang[#], Ji-chun Tan^{*}, De-zhi Su^{*}, Wen-liang Wang^{*}, Xiu-jian Li^{*}, and Hui Jia^{*}

^{*}National University of Defense Technology, Changsha, Hunan-410 073

[#]National Laboratory of Space Intelligent Control, Beijing-100 190

[†]E-mail: yuhan120483@yahoo.com.cn

ABSTRACT

Technique of measuring intensity distribution and size of spot image developed has been discussed, which is especially suitable for defocus adjustment in ground test of star tracker. A novel approach for choosing a proper defocusing position has been proposed based on collimator, Gaussian surface fitting method, and other ordinary instruments. It proves to be practical and adequate in the development of distant object tracking such as star tracker.

Keywords: Star tracker, focal adjustment, defocus, star spot image

1. INTRODUCTION

In highly accurate tracking systems, e.g., a star tracker, the image plane is commonly defocused slightly from the focal plane, spreading the spot image over several pixels of a CCD or CMOS camera, and a sub-pixel interpolation technique is used to calculate the luminance centroid of spot image¹. To determine the luminance centroid accurately, keeping the required spot size in the image plane and decreasing the variation of the spot size with the axial distance (or view angle), are highly desirable^{2,3}. Generally, the appropriate spot size is obtained by image plane defocus, and variation of spot size with a different view angle is controlled by aberrations balancing during the optical design of the lens system⁴. However, there could be many mechanisms that may cause the departure of spot intensity distribution and size from the designed, such as misalignment. Thus, the defocusing position of the image plane should be readjusted after the assembly of the lens system.

Hiroyuki⁵, *et al.* have described a technique for measuring the intensity distribution of spot image in sub-pixel resolution for star sensor. In Hiroyuki's method, the star sensor lens was installed on a two-axes rotating stage, and the star image was scanned around a certain pixel on the image sensor by rotating the stage in a 0.002 deg/pulse. The output change of this certain pixel thus represent the light intensity distribution. However, there are two issues that must be explored. The first is that the measured intensity distribution is wider than the actual one, since the scan is performed with a limited-size aperture of each pixel. The second issue is that the intensity distributions in large field angles have lower peak, as the image sensor is slightly tilted during the rotating of the lens system.

In this paper, the technique of measuring the intensity distribution and size of spot image has been developed, which is especially suitable for focal adjustment in ground test of star trackers. A novel approach for choosing a proper defocusing position has been proposed based on collimator, Gaussian surface fitting method and other ordinary instruments.

2. SIMULATED STAR IMAGE

The key issues of the focal adjustment of distant object tracking such as star tracker include the simulation of star image and spot size estimate on image sensor.

2.1 Preparation of Simulated Star Light

The real star has such a small angular size that its laboratory simulation is problematic⁶. A telescope of 1200 mm in focal length has been designed as a collimator and a small illuminated pinhole 16 μm in diameter is located just on the focal plane. White light passing through the pinhole is collimated by the collimator. The beam divergence angle due to the limited size of the pinhole aperture is very small and can be negligible.

The focal adjustment method to put the pinhole on the focal plane of the collimator lens is shown in Fig. 1. The light emitted by the simulated star is captured on real-time by a CCD camera, when shifting the penta prism. At the same time, the centroid positions of the images are obtained by sub-pixel centroid algorithm. If the simulated star light is collimated well, the centroid position will not alter during the shift of the penta prism. As the accuracy of the sub-pixel centroid algorithm is very high (usually 0.05 pixel or even better), this proposed method has the

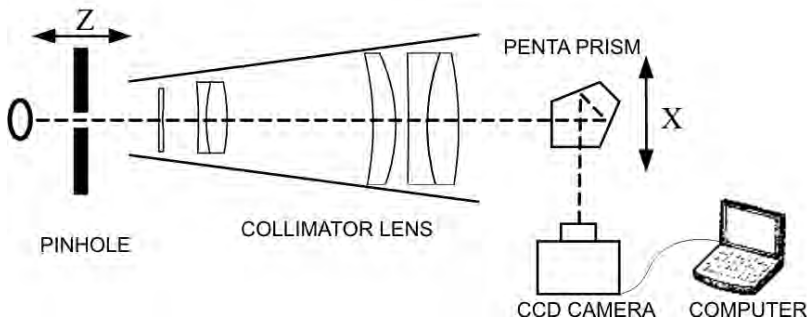


Figure 1. Adjusting method to collimate simulated star light.

characteristics of high accuracy and simplicity compared with traditional method⁷. It can satisfy the high accuracy adjustment of a single star simulator.

2.2 Simulated Star Image for Different Incident Angles of Parallel Light

The laboratory calibration setup for the focal adjustment of star tracker has been shown in Fig. 2. The collimator

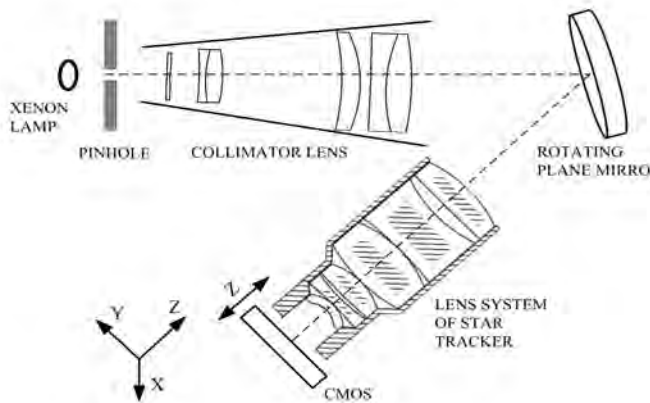


Figure 2. Star image simulation system configuration.

is placed at the front of a two-axes(X-Y) rotating plane mirror. The simulated star light reflected by the plane mirror, is captured by the star tracker lens. The incidence angle of simulated star light can be changed by adjusting the plane mirror. The interval between the lens barrel and the star tracker image detector, which is a CMOS with a resolution of 1024×1024 pixels, is adjusted by inserting pacers and fixing these by a torque screw as in the Hiroyuki's method⁵.

2.2.1 Boresight Adjustment

For simulating star image in different incident angles, the incident light must be parallel to the star tracker's boresight at first. The boresight adjustment can be performed by a laser auto collimation technique. A laser beam was placed on an adjustable stage behind the pinhole instead of the xenon lamp. Put a screen with small hole was placed between the plane mirror and the star tracker lens. The diameter of this hole was a little larger than that of the laser beam.

The first step, the stage of the laser was adjusted until the laser could illuminates approximately through the optical centre of the collimator. In the second step, the plane mirror and the screen were adjusted to make the laser light illuminate the star tracker lens through the hole of the screen. The light reflected from the optical surfaces of the star tracker lens interferes with the incident light and forms a complicated pattern around the small hole on the screen. The pattern could become symmetrical with the small hole as long as the boresight of the lens system was coincident with the laser beam⁸.

2.2.2 Simulated Star Image

When the boresight adjustment was complete, the laser and the screen were removed and the xenon lamp was turned on. At the same time, the Y and X axes graduations of the plane mirror were recovered as the zero. The collimated light originating from the xenon lamp is parallel to the boresight of star tracker in this state. That is, the simulated star image is at the point of $(0^\circ, 0^\circ)$ in Fig.3.

The star images were obtained on three points, as shown in Fig. 3 during the focal adjustment. These three measured points are expressed in rotation angles around the X-axis of the plane mirror, and these are sufficient for the focal adjustment as the lens system of star tracker is axis-symmetrical.

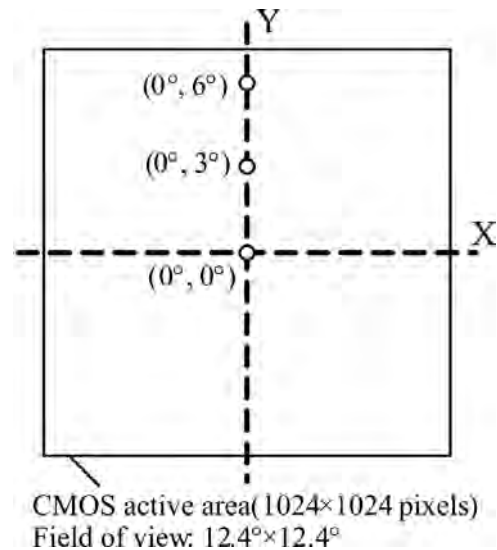


Figure 3. Measured points on CMOS.

The focal adjustment was made by inserting 10 spacer between the lens barrel and the CMOS. Then the distance between the lens barrel and the CMOS was adjusted from 3.650 mm to 3.900 mm.

3. CALCULATION OF SPOT RADIUS OF STAR IMAGE

After taking images of simulated star light, a series of image processes were performed, including star extracting and spot radius calculation.

3.1 Star Extraction

The star-extraction algorithm used consists of two basic steps. The first step is to estimate a proper threshold to separate the object signal from the background. The second step is to extract the pixels that belong to the star, and normalise these to calculate the radius of the star image spots.

3.1.1 Background Estimation

To extract the star and also measure accurately their fluxes, the background threshold should be estimated precisely.

The histogram of CMOS images obtained previously was analysed, and the distribution of the intensity values of each pixels of one CMOS image is reported in Fig. 4. Figures 4(a) and 4(b) are, the distributions of the low intensity values and high intensity values, respectively. From Fig. 4, it was found that the histogram has a peak value, and there are little pixels whose intensity values are > 20. The reason of this phenomenon is that there is only one star image spot in the whole CMOS image, and the number of pixels belonged to the star image spot can be neglected compared to the whole image pixels. So, the mean value and variance of the background can be replaced by the whole CMOS image. The background threshold can be obtained by the Wang’s method.

3.1.2 Extracted Star Pixels

Once the threshold is achieved, the intensity values of the CMOS pixels can be rewritten as Eqn (1). Then the star is extracted from the CMOS image by segmentation

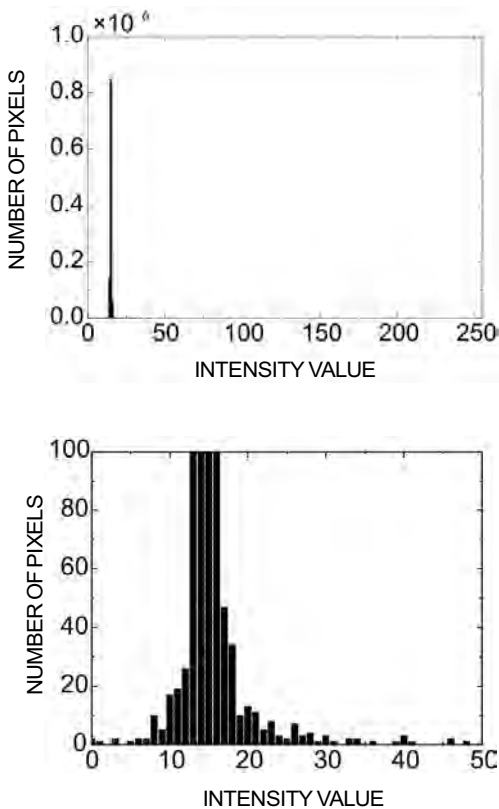


Figure 4. Histogram of CMOS star image.

with four-connection¹⁰, and the intensity values of pixels are normalised by Eqn (2) to calculate the spot radius. Actually, this normalisation is not necessary in the calculation of the spot radius. The intensity values are normalised to calculate the spot radius more conveniently.

$$g(i, j) = \begin{cases} 0, & f(i, j) \leq T \\ f(i, j) - T, & f(i, j) > T \end{cases} \quad (1)$$

where (i, j) is the position of pixel of CMOS image. $f(i, j)$ is the detected signal at pixel, and T is the background threshold obtained in Section 3.1.1.

$$g'(i, j) = \frac{g(i, j)}{\sum_{i, j} g(i, j)} \quad (2)$$

3.2 Spot Radius Calculation

For an aberration-free lens system, the point spread function (PSF) on the focal plane obtained by far-field diffraction analysis is usually a Bessel function. However, the energy distribution of star image will not be a Bessel function as the effects of the aberration and defocus. Generally, the defocused starlight is assumed to have a Gaussian distribution—a common assumption in optical applications with point sources^{2, 11}:

$$I(x, y) = \frac{I_0}{2\pi\sigma^2} \exp\left[-\frac{(x-x_c)^2 + (y-y_c)^2}{2\sigma^2}\right] \quad (3)$$

where I_0 is star integral energy of the image plane in time interval; (x_c, y_c) is centre of star image energy; σ is Gaussian dispersion radius, which corresponds with the $1/e^2$ radius. As the intensity values of pixels have been normalised, the star integral energy I_0 in Eqn (3) is 1. Thus, the normalised intensity value $g'(i, j)$ of the extracted star can be expressed as:

$$g'(i, j) = \frac{1}{2\pi\sigma^2} \exp\left[-\frac{(i-x_c)^2 + (j-y_c)^2}{2\sigma^2}\right] \quad (4)$$

By putting up the data of $g'(i, j)$ and (i, j) into the Eqn (4), the value of σ can be obtained by Levenberg-Marquardt algorithm.

4. FOCAL ADJUSTMENT

4.1 Result

The spot radius at $1/e^2$ is graphed against inserting spacer in different incident angles of parallel lights, as shown in Fig. 5.

Since this star tracker lens has a small field curvature, the graph of large incidence angle within the field of view small on the left side in the horizontal axis. The focal adjustment aims to choose an appropriate defocus position of detector image to ensure the difference of the sizes of image spot as small as possible by different incident angles. As shown in Fig. 5, the values of spot radius can not be equal for each incident angle. The aim of the focal adjustment is to balance various factors.

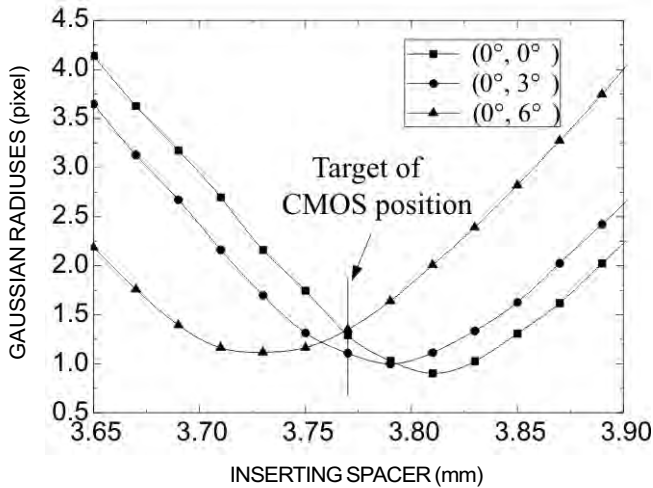


Figure 5. Spot radius changes by inserting spacer in three incident angles.

According to Fig. 5, when the inserting spacer between the lens barrel and the image sensor is 3.770 ± 0.005 mm, all fields have nearly the same value, which satisfies the target. Therefore, by setting the target of CMOS position at 3.770 mm, and the spot radius at $1/e^2$ is about 1.2 pixels.

Figure 6 shows the star spot images at various positions after the final alignment. To show the focal adjustment results approximately, the images have been zoomed in the small regions of the star image spots. Though the lower graph shows a slight coma aberration, the graph shapes at various positions are totally balanced.

4.2 Discussion

A certain pixel output, which is scanned by rotating

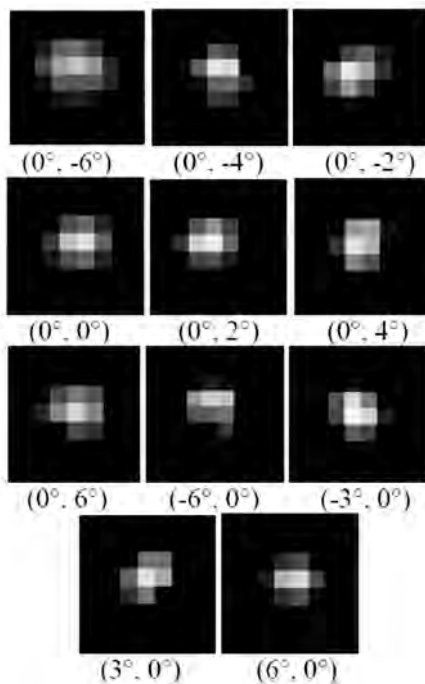


Figure 6. Image spots at various positions on the CMOS after final assembly.

the stage of the lens in a 0.002 deg/pulse, has been used to represent the light intensity distribution of the spot image in Hiroyuki's method⁵. Compared with Hiroyuki's method, the incidence angle of star light was changed by adjusting the plane mirror but not rotating the star tracker lens during the measurement in the proposed approach. Furthermore, the intensity distribution of star image was obtained directly by the detector of the star tracker, and then the spot size was calculated by Gaussian surface fitting. So the two issues mentioned in Hiroyuki's method have been explored.

The focal adjustment was made by inserting 10 spacer between the lens barrel and the CMOS. The size of inserting spacer affects the accuracy of the fitting curves in Fig. 5, but the error caused by this effect is slight and can be ignored, as the target of the focal adjustment is a range.

5. CONCLUSIONS

During the development of distant object tracking such as star tracker, the defocusing position of the image sensor should be readjusted after the assembly of lens system. This study proposes an appropriate approach to measure the intensity distribution and spot size of point-source image. Based on this scheme, the appropriate defocusing position of image sensor could be obtained. It proves to be practical and adequate in the development of distant object tracking such as star tracker.

REFERENCES

1. Liebe, C.C. Star trackers for attitude determination. *IEEE Aerosp. Electro. Syst. Mag.*, 1995, **10**(6), 10-16.
2. Hancock, B.R.; Stirbl, R.C.; Cunningham, T.J.; Pain, B.; Wrigley, C.J. & Ringold, P.G. CMOS active pixel sensor specific performance effects on star tracker/imager position accuracy. *SPIE*, 2001, **4284**, 43-53.
3. Grossman, S.B. & Emmons, R.B. Performance analysis and size optimisation of focal planes for point-source tracker algorithm applications. *Optical Engineering*, 1984, **23**(2), 167-76.
4. Liu, X.P.; Cai, X.Y.; Chang, S.D. & Grover, C.P. Bifocal optical system for distant object tracking. *Optics Express*, 2005, **13**(1), 136-41.
5. Hiroyuki, K.; Haruhiko, S.; Shoji, Y.; Miyatake, K.; Hama, K. & Nakamura, S. Optical testing of star sensor (I): Defocus spot measuring technique for ground-based test. *Optical Review*, 2008, **15**(2), 110-17.
6. Rufino, G. & Moccia, A. Stellar scene simulation for indoor calibration of modern star trackers. *Space Technology*, 2001, **21**(1-2), 41-51.
7. He, H.H.; Ye, L.; Zhou, X.Y. & Shen, X.H. Theory and precision analysis of testing apparatus of parallel depth. *Opto-Electronic Engineering*, 2007, **34**(5), 52-6 (Chinese).
8. Xing, F.; Dong, Y. & You, Z. Laboratory calibration of star tracker with brightness independent star identification strategy. *Optical Engineering*, 2006,

45(6), 63601-3604.

9. Wang, Z.K. & Zhang, Y.L. Algorithm for CCD star image rapid locating. *Space Science*, 2006, **26**(3), 209-14 (Chinese).
10. Jiang, Y.L.; Zhang, G.J.; Li, X. & Wei, X.G. A fast star tracking algorithm for star sensor. *Acta Aeronautica et Astronautica Sinica*, 2006, **27**(5), 913-16 (Chinese).
11. Liebe, C.C. Accuracy performance of star trackers - A tutorial. *IEEE Trans. Aerosp. Electro. Syst.* 2002, **38**(2), 587-99.

Contributors



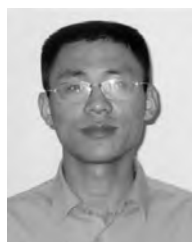
Mr Hai-bo Liu obtained his MS from National University of Defence Technology in 2008. His research interests are optics and photoelectricity measurement.



Mr Jian-kun Yang obtained his MS (Optical Engineering) from National University of Defence Technology, China, in 1993. Presently, working as a Professor at College of Science, National University of Defence Technology. His research areas include optical information procession, automatic target recognition, and remote sensing.



Mr Ji-chun Tan obtained his MS from Sichuan University in 1984. Presently, working as a Professor at College of Science, National University of Defence Technology. His research areas are photoelectricity measurement, and image processing and volume grating.



Mr De-zhi Su obtained his BS from National University of Defence Technology, China, in 2008. His research areas are optics, and photo electricity measurement.



Mr Wen-liang Wang obtained his BS from the National University of Defence Technology, China, in 2008. His research areas are opto-electrical technology, and space measurement.



Mr Xiu-jian Li obtained his PhD in Optical Engineering from the National University of Defence Technology, China, in 2007. Currently, working as an Associate Professor at College of Science, National University of Defence Technology. His research areas include optical information procession, and optical computing.



Mr Hui Jia obtained his BS (Applied Physics) from the National University of Defence Technology, China, in 2005. His research areas include optical information procession, and optical computing.